NeuroImage 125 (2016) 724–730

Contents lists available at ScienceDirect

NeuroImage

journal homepage: www.elsevier.com/locate/ynimg

GABA concentration in superior temporal sulcus predicts gamma power and perception in the sound-induced flash illusion

Johanna Balz [a], Julian Keil [a], Yadira Roa Romero [a], Ralf Mekle [b], Florian Schubert [b], Semiha Aydin [b], Bernd Ittermann [b], Jürgen Gallinat [c], Daniel Senkowski [a,*]

[a] Department of Psychiatry and Psychotherapy, Charité - Universitätsmedizin Berlin, Große Hamburger Straße 5-11, 10115 Berlin, Germany
[b] Physikalisch-Technische Bundesanstalt (PTB), Abbestraße 2-12, 10587 Berlin, Germany
[c] Department of Psychiatry and Psychotherapy, Universitätsklinikum Hamburg-Eppendorf, Martinistraße 52, 20246 Hamburg, Germany

ARTICLE INFO

Article history:
Received 8 October 2015
Accepted 31 October 2015
Available online 4 November 2015

Keywords:
Multisensory
Oscillatory activity
Gamma-aminobutyric acid
Glutamate
Magnetic resonance spectroscopy
Electroencephalography

ABSTRACT

In everyday life we are confronted with inputs of multisensory stimuli that need to be integrated across our senses. Individuals vary considerably in how they integrate multisensory information, yet the neurochemical foundations underlying this variability are not well understood. Neural oscillations, especially in the gamma band (>30 Hz) play an important role in multisensory processing. Furthermore, gamma-aminobutyric acid (GABA) neurotransmission contributes to the generation of gamma band oscillations (GBO), which can be sustained by activation of metabotropic glutamate receptors. Hence, differences in the GABA and glutamate systems might contribute to individual differences in multisensory processing. In this combined magnetic resonance spectroscopy and electroencephalography study, we examined the relationships between GABA and glutamate concentrations in the superior temporal sulcus (STS), source localized GBO, and illusion rate in the sound-induced flash illusion (SIFI). In 39 human volunteers we found robust relationships between GABA concentration, GBO power, and the SIFI perception rate (r-values = 0.44 to 0.53). The correlation between GBO power and SIFI perception rate was about twofold higher when the modulating influence of the GABA level was included in the analysis as compared to when it was excluded. No significant effects were obtained for glutamate concentration. Our study suggests that the GABA level shapes individual differences in audiovisual perception through its modulating influence on GBO. GABA neurotransmission could be a promising target for treatment interventions of multisensory processing deficits in clinical populations, such as schizophrenia or autism.

Introduction

Ever since researchers have investigated multisensory integration phenomena, they have reported a high variability between individuals (Urbantschitsch, 1888). This variability might be due to individual differences in local information processing and large-scale interplay between brain regions. A number of recent studies suggested that neural oscillations, especially in the gamma band, play an important role therein (Kayser and Logothetis, 2009; Lakatos et al., 2007; Lange et al., 2011; Senkowski et al., 2008; Van Atteveldt et al., 2014). Furthermore, Gamma-aminobutyric acid (GABA) neurotransmission has been shown to contribute to the generation of gamma band oscillations (GBO) (Bartos et al., 2007; Buzsáki and Wang, 2012; Sohal et al., 2009; Traub et al., 2003). Moreover, GBO can be driven by activation of metabotropic glutamate receptors (Bartos et al., 2007; Whittington et al., 1995). Together, these findings indicate a three-way relationship between the GABA and glutamate systems, GBO, and multisensory processing.

A multisensory paradigm in which GBO modulations have been consistently found is the sound-induced flash illusion (SIFI) (Bhattacharya et al., 2002; Mishra et al., 2007). In this paradigm, multiple auditory stimuli that are presented alongside a single visual stimulus can induce illusory percepts of multiple visual stimuli (Shams et al., 2000). Individuals substantially vary in the number of illusions that they perceive in the SIFI. For this reason, the SIFI is ideally suited for examining the neurochemical and neurophysiological foundations underlying individual differences in audiovisual perception. Magnetic resonance spectroscopy (MRS) is an established method for obtaining resting GABA (Edden et al., 2012; Mescher et al., 1998) and glutamate (Mekle et al., 2009; Mlynarik et al., 2006) concentrations in selected brain regions. GABA concentration has been shown to be related to visual perception (Edden et al., 2009; Van Loon et al., 2013). Moreover, a highly cited study has revealed a positive relationship between GABA concentration in the visual cortex and individual GBO peak frequency (Muthukumaraswamy et al., 2009), but recent data have challenged this finding (Cousijn et al., 2014). In

* Corresponding author at: Dept. of Psychiatry and Psychotherapy, Charité - Universitätsmedizin Berlin, St. Hedwig Hospital, Große Hamburger Str. 5-11, 10115 Berlin, Germany. Fax: +49 30 2311 2209.
E-mail address: daniel.senkowski@charite.de (D. Senkowski).

http://dx.doi.org/10.1016/j.neuroimage.2015.10.087
1053-8119/

addition, a recent visual repetition priming study has shown a positive relationship between the event-related glutamate level in the lateral occipital cortex and the amplitude of evoked GBO (Lally et al., 2014). In the present study, we measured MRS and EEG to test whether the GABA and glutamate systems account for individual differences in multisensory processing via their influence on GBO. GABA and glutamate concentrations were obtained from a voxel in the superior temporal sulcus (STS) — a key area in multisensory processing (Beauchamp et al., 2004; Calvert, 2001; Noesselt et al., 2007).

Material and methods

Participants and stimuli

Forty volunteers participated in the study. One of them was excluded from further analysis because he did not perceive the illusion. The mean age of the remaining 39 participants (17 female; 37 right-handed) was 32.8 years (range: 18–51 years). They had normal hearing and normal or corrected-to-normal vision, and reported no history of neurological or psychiatric disorders. EEG and MRS data were acquired on separate days within 48 hours. The study was conducted in accordance with the Declaration of Helsinki and approved by the ethics committee of the Charité – Universitätsmedizin Berlin. Participants provided written informed consent. The SIFI experiment was conducted in a sound-attenuated electrically shielded chamber. Stimuli were presented on a CRT monitor with a background luminance of 21 cd/m^2. Six stimulus combinations were presented, consisting of 0, 1 or 2 auditory (A) stimuli combined with either 0, 1 or 2 visual (V) stimuli (A_0V_1, A_0V_2, A_1V_1, A_2V_0, A_2V_1, A_2V_2) (Fig. 1). Each visual stimulus was presented for 10 ms and consisted of a white disk subtending a visual angle of 1.6° with a luminance of 89 cd/m^2. Visual stimuli were presented at 4.1° centrally below the fixation cross. Each auditory stimulus was presented for 7 ms and consisted of a 73 dB (SPL) 1000 Hz sine wave tone. The presentation of auditory inputs at equal physical sound–pressure level rather than equal subjectively perceived loudness is permissible since the influence of auditory stimulus intensity on the SIFI illusion rate is relatively small (Andersen et al., 2004). Auditory stimuli were presented from a central speaker below the screen. The participants' task was to report the number of perceived visual stimuli by pressing a button with the index, middle, or ring finger of their right hand to indicate whether they perceived zero, one, or two flashes, respectively. Three hundred SIFI trials and 150 trials per control condition were presented in random order in eight blocks. The total experimental runtime was 44 minutes. Additionally, short breaks were included after each block.

EEG methods

EEG was recorded using a 128-channel active system (EasyCap, Herrsching, Germany), including one horizontal and one vertical EOG electrode. Data were recorded against nose reference with a pass band (0.016–250 Hz) and digitized at a sampling rate of 1000 Hz. Preprocessing and offline data analysis were performed using EEGlab (Delorme and Makeig, 2004), Fieldtrip (Oostenveld et al., 2011), and custom-made Matlab scripts (MathWorks, Natick, MA). Data were offline high-pass filtered (1 Hz, FIR), low-pass filtered (125 Hz, FIR), and notch-filtered (49.1–50.2 Hz, 4th order two-pass Butterworth filter). Moreover, data were down-sampled to 500 Hz.

Epochs (−1 to 3 s around stimulus onset) of A_2V_1 trials in which participants perceived one or two flashes were extracted and those containing muscular artefacts were rejected by visual inspection. Trials containing remaining artefacts with amplitudes of ±100 μV were rejected automatically, and independent component analysis was conducted to correct for EOG and ECG artefacts. On average, 15.35 ± 6.26 (SD) independent components were rejected. Next, noisy channels were interpolated using spherical interpolation (average 1.5 ± 1.54 (SD)

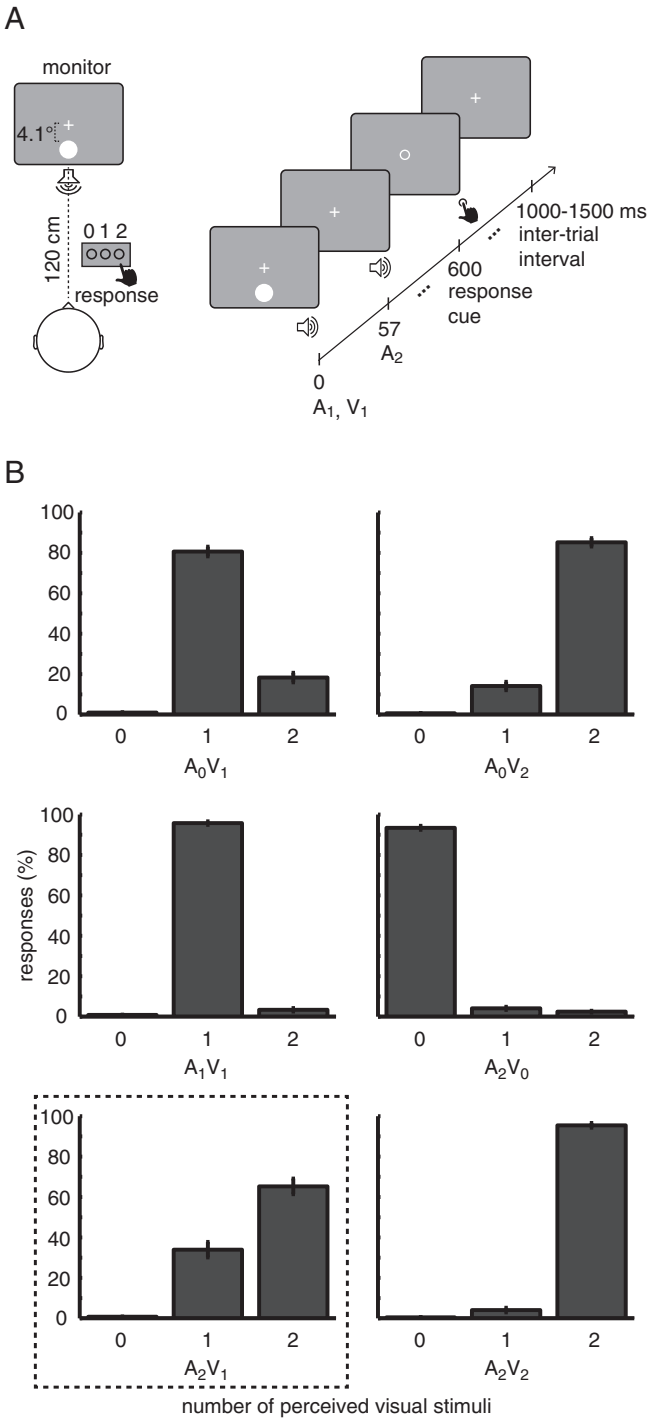

Fig. 1. Experimental setup and behavioral data for the six stimulus types in the sound-induced flash illusion paradigm. (A) Left panel: Participants fixated a central white cross while being presented with stimuli of the sound-induced flash illusion paradigm. A single flash presented alongside two rapidly repeating tones is either perceived as one or two flashes. Right panel: Timeline of the critical A_2V_1 trial, in which participants frequently perceived two visual inputs. The visual stimulus and the first auditory stimulus were presented simultaneously. The second auditory stimulus was presented 57 ms after the onset of the first stimulus. Six hundred milliseconds after the onset of the first stimulus, the fixation cross was replaced by a response cue, which comprised an empty circle that was presented in the center of the screen. (B) The indexed numbers denote the number of auditory (A) and visual (V) inputs in the six different stimulus types (e.g., two auditory inputs were presented together with two visual inputs in A_2V_2 trials). The gray bars denote the numbers of perceived visual stimuli (with SEM). Participants reported perceiving two flashes in 64% of the critical A_2V_1 trials (highlighted in a box).

channels). Finally, data were re-referenced to the common average. For the GBO analysis of combined illusion and no illusion A_2V_1 trials we applied similar procedures as in a recent study on the relationships between GBO and resting transmitter concentrations (Cousijn et al., 2014). On the sensor level, time–frequency analysis (40 to 80 Hz, in 0.5 Hz steps) was performed using a sliding window multitaper convolution transformation with discrete prolate spheroidal (slepian) taper sequences with a length of 400 ms (frequency smoothing ±5 Hz, 10 ms temporal resolution). Power was normalized to reflect the relative change from the −600 to −200 ms baseline period and tested for significant modulations against zero using a cluster corrected nonparametric t-test with Monte-Carlo randomization (Maris and Oostenveld, 2007). Using individual T1-weighted structural MRIs, realistic three-shell boundary element models were constructed. For the leadfield computation, a template grid of cortical sources with a 1 cm resolution was created based on the MNI-brain and warped to the individual head size for the source analyses. For the source projection, we calculated the covariance matrix between all sensor pairs of averaged band-passed filtered (40–80 Hz, 2nd order Butterworth filter) single trials. The ROI for the correlation was established from the overlap of the AAL atlas region labeled as "Temporal Sup L" (Tzourio-Mazoyer et al., 2002) and the MRS box, i.e., we chose the virtual channels that were localized within the STS and within the 3 × 3 × 2 box of the MRS voxel. A linearly constrained minimum variance beamformer (LCMV) (Van Veen et al., 1997) was applied to compute individual spatial filters for each participant using this covariance matrix. The lambda regularization-parameter was set to 10%. The spatial filters were then multiplied with the unfiltered sensor level time series to reconstruct source level raw time series for each cortical source resulting in virtual electrodes (Cousijn et al., 2014; Keil et al., 2014). Finally, we computed the same time–frequency analysis as on the sensor level. To visualize the cortical source of sensor-level GBO, we computed an FFT centered on the peak power of the average GBO in the 200 to 600 ms post-stimulus interval (65 Hz, frequency smoothing ±6 Hz). We used dynamic imaging of coherent sources (Gross et al., 2001) to identify the cortical source of this effect by contrasting source-localized power with the noise estimate. The anatomical regions of the source localization were determined based on the AAL atlas.

MR methods

MR images and spectra were collected on a 3 T Verio (Siemens Healthcare, Erlangen, Germany). Anatomical images were acquired using a three-dimensional T1-weighted magnetization prepared gradient-echo sequence (MPRAGE) with an isotropic resolution of 1.0 mm, a repetition time (TR) of 2.3 s, an echo time (TE) of 3.03 ms, an inversion time (TI) of 900 ms, and a flip angle of 9°. The volume of interest (VOI = 20 × 30 × 20 mm^3) for single voxel MRS, encompassing the left STS, was positioned below the upper bank of the temporal cortex. The transmitter radiofrequency (RF) voltage was calibrated for the individual VOI, followed by adjustment of first- and second-order shims using FAST(EST)MAP. First, GABA-edited spectra were measured using MEGA-PRESS (Edden et al., 2012; Mescher et al., 1998) with number of acquisitions (NA) = 256, TR = 3.0 s, and TE = 68 ms. Due to its editing scheme, MEGA-PRESS permits the detection of a selected molecular species with excellent selectivity and good sensitivity. In the present experiments, the editing pulse was applied at 1.9 ppm in alternate scans thus allowing the reliable detection of the GABA pseudo-triplet at 3.0 ppm. Following this scan, a spectrum without water suppression was recorded (NA = 8). Immediately afterwards, spin echo full intensity acquired localized (SPECIAL) spectra were acquired from the same voxel. The short echo time of the SPECIAL sequence enables the determination of a large number of metabolites and yields a high precision for the detection of glutamate (Mlynarik et al., 2006; Mekle et al., 2009; Near et al., 2013). The sequence was used with water suppression by VAPOR (variable power radio frequency pulses with optimized relaxation delays) and six outer volume suppression slices placed around the spectroscopic voxel to saturate outside spins. For each metabolite spectrum, the NA was 256 with TR = 3 s and TE = 8.5 ms. Following this scan, a spectrum without water suppression was recorded (NA = 8).

If the water line width calculated from a fit to a water spectrum acquired after shimming was greater than or equal to 9.5 Hz, all corresponding MRS data were not used for further analysis. The mean water line width (±standard deviation) of the remaining dataset (n = 37) was determined to be 7.8 (±0.7) Hz. For the analysis of the SPECIAL data, the spectra were corrected for frequency drift during acquisition and analyzed using LCModel (Provencher, 1993) with a simulated basis set containing 20 metabolites.

The unsuppressed water spectrum was used for eddy current correction and referencing the metabolite spectrum to the internal water concentration. Edited MEGA-PRESS spectra were analyzed using LCModel with a measured basis set containing GABA, N-acetylaspartate (NAA), glutamate (Glu), glutamine (Gln), and glutathione, and referenced to the GABA concentration used for creating the basis set. Only those GABA amplitudes with Cramér-Rao lower bounds (CRLB) below 25%, as returned by LCModel (Provencher, 1993), were used for further analysis. Three GABA values did not fulfill this criterion and were therefore removed. Of the remaining data, CRLB of the LCModel fits were 12.1 ± 3.2% for GABA (n = 34) and 4.3 ± 1.0% for glutamate (n = 37). Metabolite amplitudes were corrected for relaxation using T1 and T2 values at 3 T. To correct the in vivo concentrations for the amount of cerebrospinal fluid (CSF) in the selected VOI, segmentation of the T1-weighted images was performed using statistical parametric mapping (SPM8). Pixels in the VOI were classified according to their probability calculated by SPM8 to belong to one of the tissue types: CSF, gray matter, or white matter. Note that the CSF fraction in STS is very small, permitting us to neglect errors in CSF estimation caused by the small chemical displacement of the metabolites and imperfections of RF pulse profiles. The average glutamate and GABA concentrations calculated in this manner were 8.53 ± 1.16 mmol/l and 1.40 ± 0.35 mmol/l, respectively.

Results

Participants reported illusory percepts of two flashes in 10% to 99% of the critical SIFI trials, where a single flash is accompanied by two rapidly repeating tones. Behavioral data for five other stimulus types, which served as control trials, showed that participants were able to correctly distinguish between one and two flashes (Fig. 1B). To examine whether the illusion of two flashes was specific to the SIFI trials, we compared the reports of two flashes between the critical A_2V_1 with the A_0V_1 and A_1V_1 conditions. The percept of two flashes was significantly higher in A_2V_1 trials (65%) compared with A_0V_1 (18%; $t(38) = 6.636$, $p < 0.001$) and A_1V_1(3%; $t(38) = 12.904$, $p < 0.001$) trials. This demonstrates that the illusion effect is specific to SIFI trials.

To further investigate whether a response bias could have contributed to the present data, we correlated the percentage of trials in which participants perceived two flashes in the control conditions with the illusion rate in A_2V_1 trials. For this analysis we set a Bonferroni corrected alpha level of 0.05/5 = 0.01. The analyses revealed significant relationships between A_0V_2 and A_2V_1 conditions ($r = 0.478$, $p = 0.002$), as well as between A_2V_2 and A_2V_1 conditions ($r = 0.602$, $p < 0.001$). There were no significant correlations for the other three control conditions. Hence, participants who perceived more often two flashes in the A_0V_2 and A_2V_2 conditions also perceived more illusions in A_2V_1 trials. Notably, there were no relationships between illusion rates and conditions in which only one visual stimulus was presented. This lack of relationships argues against a simple response bias.

For the analysis of neural oscillations, we followed the procedure of a recent study investigating the relationships between neurotransmitter concentration and GBO (Cousijn et al., 2014). In SIFI trials, we compared

gamma band power (40–80 Hz) between the post-stimulus interval and the baseline. We found robust GBO power enhancements at the scalp level (Fig. 2A–B). These enhancements were most pronounced at central electrodes, but the topography plot also indicates some GBO modulations at frontal and temporal sites. However, the only electrode cluster that revealed significant poststimulus vs. prestimulus GBO modulations was found at central electrodes (mean t-value of the significant cluster: $t(38) = 3.101$, $p = .02$; highlighted bold dots in Fig. 2A). Using beamformer source analysis (Gross et al., 2001; Van Veen et al., 1997), GBO power was localized in the STS and extrastriate cortex of the left hemisphere with the peak of activation in the AAL atlas area "Temporal Sup L" (Fig. 2C). The individual peak frequency in the 40 to 80 Hz range and its corresponding power were calculated for the 200 to 600 ms post-stimulus period. This was done across source grid points corresponding to the STS volume targeted by the MRS acquisition (Fig. 3).

For the quantification of the weak GABA signal we used the highly selective MRS pulse sequence MEGA-PRESS, which is widely considered to be the sequence of choice for measuring this neurotransmitter in 3 T-MRS (Edden et al., 2012; Mescher et al., 1998) The glutamate concentration can be also robustly determined with other sequences, and we used SPECIAL (Mekle et al., 2009; Mlynarik et al., 2006), which especially at short echo time, offers a high signal-to-noise ratio. Concentrations were quantified from spectra using a linear combination model (Provencher, 1993). Data were corrected for relaxation and individual cerebrospinal fluid content of the examined volume element. Fig. 3 illustrates typical SPECIAL and MEGA-PRESS spectra together with the residuals, background fits, and fits for glutamate and GABA.

Pearson correlation coefficients were computed for each pair in the triangle of neurotransmitter concentrations (GABA or glutamate), GBO (power or frequency), and SIFI illusion rates. We used Holm–Bonferroni corrected significance thresholds to account for multiple comparisons. GBO power and GABA concentration significantly correlated with the SIFI illusion rate ($r = 0.438$, $p = 0.005$, Fig. 4A, and $r = 0.469$, $p = 0.005$, Fig. 4B, respectively). Moreover, we found a highly significant correlation between GABA concentration and GBO power ($r = 0.532$, $p = 0.001$, Fig. 4C). The relationships remained significant when age of participants and gray matter volume in the STS voxel were used as covariates in partial correlation analyses (all p-values < 0.007). Next, we computed a path model analysis (Buckholtz et al., 2010) and found that the correlation between GBO power and SIFI illusion rate is about twofold higher when GABA concentration is included as compared to when it is excluded (Fig. 4D). The bootstrapping test with 1000 samples revealed a bias-corrected confidence interval of 1.954 to 242.2. While not being a proof of causality, this finding establishes a mediating effect of the GABA level on the relationship between GBO power and the SIFI illusion rate. No significant correlations were found with respect to individual GBO peak frequency or glutamate concentration (Table 1). Finally, we calculated Bayes factors (BF) which summarize the ratio of evidence for a correlation versus the evidence for a null hypothesis of no correlation (Wetzels and Wagenmakers, 2012). The analysis

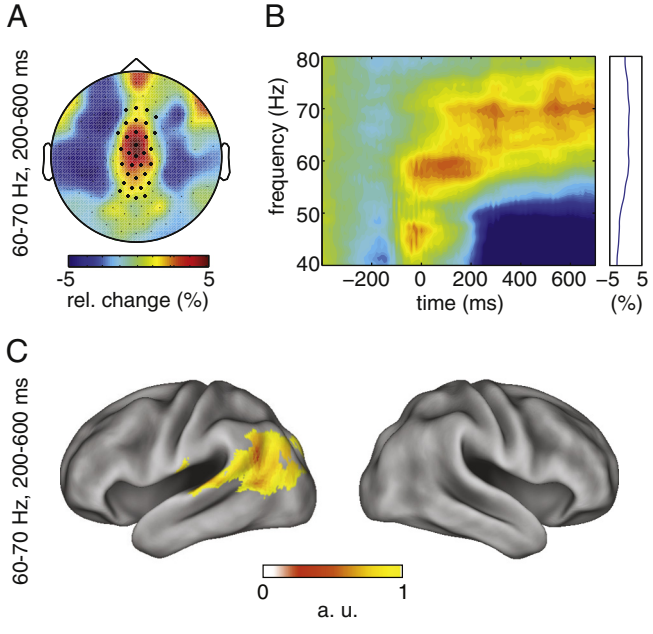

Fig. 2. Gamma band oscillations in the sound-induced flash illusion. (A) Topography of GBO power change in response to SIFI stimuli, in which a single flash is presented alongside two rapidly repeating tones. The bold dots highlight the cluster of electrodes for which a significant post-stimulus power increase relative to baseline was found in the 200 to 600 ms period. (B) Time–frequency representation of relative power changes for the central electrode cluster depicted in (C). (C) GBO power was source-localized in the left STS and extrastriate cortex. The figure was masked at a 0.85 threshold relative to the maximum. a.u. = arbitrary units.

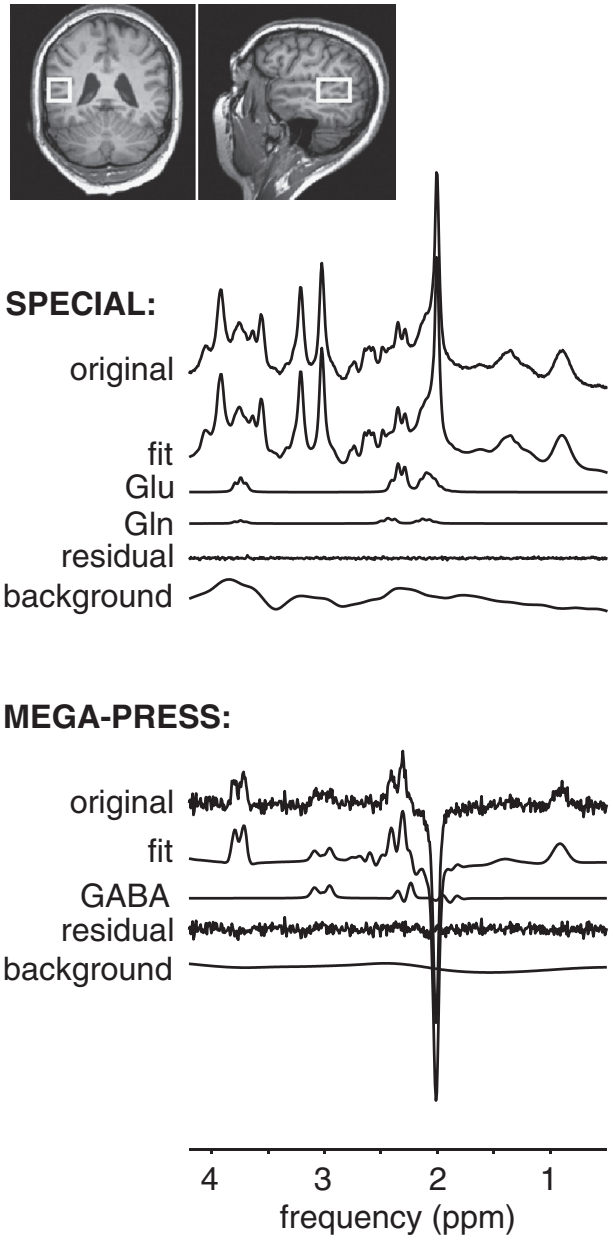

Fig. 3. Sample magnetic resonance spectra from the left STS voxel. The upper panel illustrates the location of the voxel on T1-weighted images. The top row of each panel represents the original SPECIAL or MEGA-PRESS spectrum, respectively. Also shown are the overall fits and the fitted components of interest, as well as the background. The small residuals reflect the high quality of the fits.

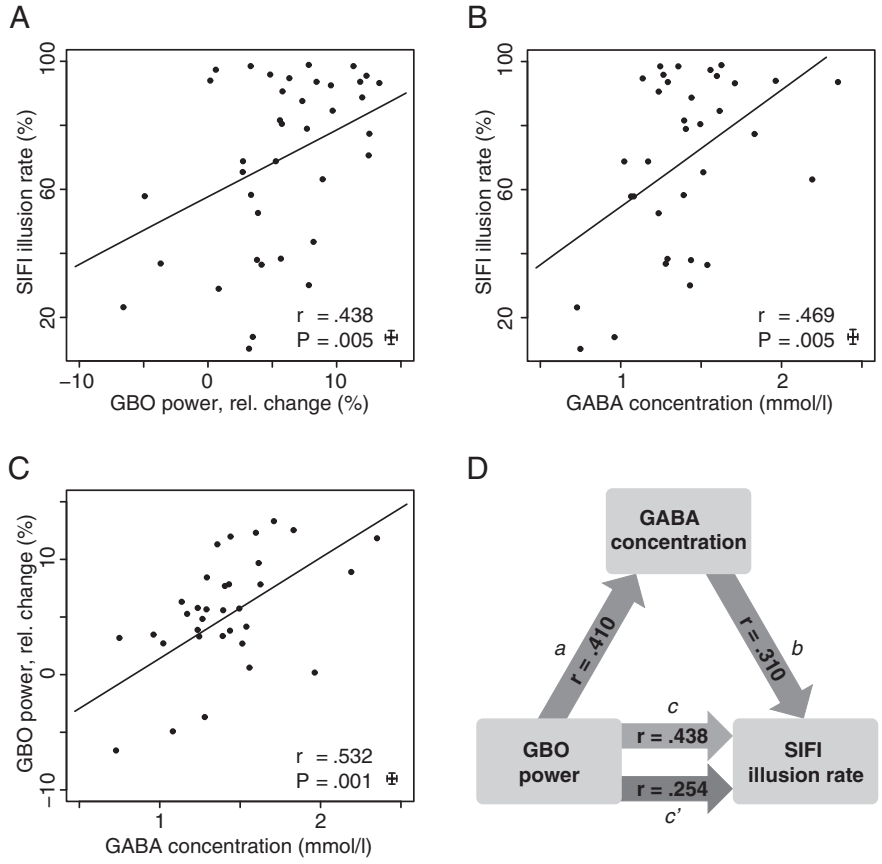

Fig. 4. GABA concentration shapes audiovisual perception via its influence on gamma band oscillations. (A) Source-localized GBO power in the STS is positively correlated with the SIFI illusion rate (N = 39). (B) and (C) GABA concentration in the STS correlates with SIFI illusion rate and GBO power, respectively (N = 34). (D) Path analysis reveals that GABA concentration mediates the positive correlation between GBO and the SIFI illusion rate. Path *a* reflects the coefficient for the effect of GBO power on GABA concentration. Path *b* reflects the coefficient for the effect of GABA concentration on the illusion rate. Paths *c* and *c*′ reflect the coefficients for the total and direct effects (i.e., with (*c*) and without (*c*′) the contribution from GABA) of GBO on SIFI illusion rate, respectively. A bootstrapping test, which involved 34 participants for whom all three measures were available, revealed significant differences between the effects of paths *c* and *c*′.

provided further evidence for the correlations between GABA concentration, GBO power, and multisensory perception, as well as for the null hypothesis in all other correlations (Table 1). It is possible that the correlation between GBO power and the perception of two flashes in SIFI trials was not specific to the illusion percept per se, but could also be found in other conditions that contained two flashes. To address this question, we correlated the GBO power in response to A_0V_2 trials with the percentage of two flashes reports in this condition. This analysis revealed no significant relationship ($r = -0.143$, $p = 0.385$), suggesting that the correlation between GBO power and the SIFI illusion is linked to the illusory percept of two flashes. Finally, a previous study has reported that the prestimulus GBO was correlated with the double-flash illusion in a visuotactile paradigm (Lange et al., 2013). In accordance with this report, we correlated the source-localized baseline GBO power with the SIFI illusion rate but did not find a significant relationship ($r = -0.062$, $p = 0.705$). Additionally, we correlated the source-localized baseline GBO power with the GABA level but did not find a relationship ($r = -0.146$, $p = 0.408$).

Discussion

We examined the neurochemical and neurophysiological foundations underlying individual differences in audiovisual perception. Our study revealed several important findings. Firstly, the GBO power correlated positively with the illusion rate in the SIFI. In addition to the SIFI paradigm (Bhattacharya et al., 2002; Mishra et al., 2007), GBO

Table 1
Overview of Pearson correlations and corresponding Bayes factors (BF).

	No. of subjects	Pearson's r	p-Value	Bayes factor
GBO power × SIFI illusion rate	39	0.438	**0.005**	**5.91**
GBO peak frequency × SIFI illusion rate	39	−0.076	0.645	0.14
GABA concentration × SIFI illusion rate	34	0.469	**0.005**	**6.46**
GABA concentration × GBO power	34	0.532	**0.001**	**24.08**
GABA concentration × GBO peak frequency	34	−0.068	0.704	0.14
Glutamate concentration × SIFI illusion rate	37	−0.122	0.473	0.17
Glutamate concentration × GBO peak frequency	37	−0.155	0.359	0.19
Glutamate concentration × GBO power	37	−0.174	0.304	0.22

The BFs provided substantial (BF = 3–10) or strong (BF = 10–30) evidence for H_1 in all significant correlations (highlighted in bold). The BFs of the non-significant correlations provided substantial (BF = 0.1–0.33) or anecdotal (BF = 0.33–1) evidence for the null hypothesis. GBO = gamma band oscillations, SIFI = sound-induced flash illusion. Note that only 37 values for glutamate and 34 values for GABA fulfilled the quality criteria for MR spectra (see the Materials and Methods section).

modulations have been reported in other audiovisual paradigms, such as the motion-bounce (Hipp et al., 2011) and the McGurk illusion (Kaiser et al., 2005). This provides strong evidence for a role of GBO in audiovisual perception. The GBO in our study was found in a similar frequency, latency, and in comparable cortical regions as observed for semantic matching in crossmodal haptic-to-auditory priming (Schneider et al., 2011). Specifically, the GBO was source localized in the left STS, which has been frequently related to integrative audiovisual processing (Hipp et al., 2011; Kaiser et al., 2005; Van Loon et al., 2013). For instance, using transcranial magnetic stimulation, Beauchamp et al. (2010) showed that temporary disruption of the left STS reduces the perception rate of the McGurk illusion. Moreover, a recent functional magnetic resonance imaging study revealed a positive relationship between the blood oxygenation level dependent contrast in the left STS and the likelihood of perceiving the McGurk illusion (Nath and Beauchamp, 2012). Taken together, current evidence suggests that differences in stimulus processing in the left STS contribute to individual differences in audiovisual perception.

A second key finding in our study is a strong positive relationship between GABA concentration and GBO power in the STS. GABA concentration accounted for 28% (i.e., $r = 0.532$) of the individual variability in GBO power. In line with data from animal studies (Sohal et al., 2009; Traub et al., 2003) and human pharmacological investigations (Lozano-Soldevilla et al., 2014), this suggests that the GABA system has a modulatory influence on GBO power. We did not observe a relationship between GABA concentration and GBO peak frequency in the STS, as it was previously discussed for the visual cortex. A magnetoencephalography study conducted in a small sample found a positive relationship between GABA concentration in the visual cortex and the peak frequency of GBO in response to visual motion stimuli (Muthukumaraswamy et al., 2009). However, a recent study in a larger sample did not replicate this finding (Cousijn et al., 2014). Our own results reinforce the notion that there is no close relationship between the GABA level, obtained by MRS, and GBO peak frequency. The two studies differed from our study in respect to the investigated brain regions, experimental tasks, and partially in MRS protocols. In the present study, we used the MRS pulse sequence MEGA-PRESS, which is tailored to the detection of the GABA pseudo-triplet at 3 ppm (Edden et al., 2012). Moreover, we examined a multisensory illusion paradigm that robustly induces GBO (Bhattacharya et al., 2002; Mishra et al., 2007). In line with a previous combined MRS-MEG study by Cousijn et al. (2014), we investigated both the power and frequency of GBO. We found that GABA concentration in the STS predicts the power, but not the frequency of GBO during audiovisual perception. Our observation differs from the result obtained by Cousijn et al. (2014), who did not find significant correlations between GABA level and GBO power. The differences in experimental tasks and examined cortical regions might have contributed to the different outcomes.

A third key finding is a positive relationship between GABA concentration and the individual likelihood to perceive the SIFI. Previous studies have revealed that the GABA level in the visual cortex is correlated with unisensory visual perception. Edden et al. (2009) demonstrated that GABA concentration in the visual cortex predicts the individual performance in a visual orientation discrimination task. More recently, Van Loon et al. (2013) showed that GABA concentration in the visual cortex also relates to a reduced number of perceptual switches and lengthening of percept durations in bistable visual perception. Our findings extend these observations by demonstrating that the GABA level in a higher polysensory area predicts individual differences in audiovisual perception. Furthermore, our observation that the GABA system plays a role in audiovisual processing is in agreement with data from a recent animal study using in vivo whole-cell recordings (Iurilli et al., 2012). Iurilli et al. (2012) demonstrated a crossmodal influence of the auditory cortex on inhibitory GABAergic circuits in the primary visual cortex. Furthermore, the maturation of GABA circuits is believed to be an important factor for the emergence of multisensory integration properties in the cortex (Gogolla et al., 2014). In summary, evidence from various studies suggests that the GABA system plays a crucial role in multisensory integration.

In contrast to GABA, we did not find relationships of the glutamate level with GBO and audiovisual perception. While in vitro studies have shown that activation of metabotropic glutamate receptors can drive GBO in the hippocampus (Whittington et al., 1995), the glutamate level in the present study might not have contributed to individual differences in GBO power and audiovisual perception. It is possible that the glutamate level is not a sensitive measure for specific aspects of glutamate-mediated neurotransmission that might affect audiovisual perception. Physiologically, the individual variability in neurotransmitter concentrations as obtained by MRS could be due to various parameters, such as differences in the number of neurons, the number of synapses per neuron, or the concentration per neuron (Sumner et al., 2010). How these parameters relate to audiovisual perception and whether the glutamate system contributes to individual differences in audiovisual perception is unknown.

Finally, for the interpretation of results it is important to consider how GABA acts at the synaptic level. GABA plays a crucial role for the finely tuned excitation/inhibition (E/I) balance in neural populations, which is essential for the generation of GBO (Attalah and Scanziani, 2009; Isaacson and Scanziani, 2011; Ursino et al., 2010). For instance, a model of impaired GABAergic dendritic inhibition can explain epileptic fast activity (Wendling et al., 2002). The E/I balance is also relevant for binding processes underlying unisensory perception (Wang, 2010). In a similar vein, the E/I balance might also contribute to the integration of multisensory information (Senkowski et al., 2008; Van Atteveldt et al., 2014). Hence, in the case of a suboptimal E/I balance, which results in an inefficient generation and modulation of GBO, multisensory integration processes might be also less efficient. Poor GABA-mediated neurotransmission at the synaptic level might have also contributed to the finding that individuals with low GABA levels in the STS expressed reduced GBO power and lower multisensory illusion rates. How the GABA level, as obtained by MRS, actually relates to GABAergic neurotransmission at the synaptic level remains to be elucidated.

Conclusion

The key novel finding of our study is that the GABA level in the STS mediates the positive relationship between GBO and audiovisual perception. Previous studies have provided strong evidence for the role of GBO in multisensory processing (Hipp et al., 2011; Lakatos et al., 2007; Senkowski et al., 2011). In addition, it is known that the GABA system is involved in the generation of GBO (Bartos et al., 2007; Sohal et al., 2009; Traub et al., 2003; Wang, 2010). The present study is the first that investigated the complete triangle, and which established a robust three-way relationship between the GABA level, GBO, and audiovisual perception. This finding has implications for the treatment of individuals with multisensory processing deficits. Dysfunctional multisensory processing (Brandwein et al., 2013; Ross et al., 2007) as well as alterations in the GABA system (Uhlhaas and Singer, 2012) have been found in psychiatric disorders, such as schizophrenia and autism spectrum disorder. GABA-mediated neurotransmission may be essential for balancing neural excitation and inhibition during multisensory integration (Hoshino, 2012, 2014). Thus, alterations in the GABA system might contribute to multisensory processing deficits in schizophrenia (Cloke and Winters, 2015) and autism (Gogolla et al., 2014). Together with the present data, this suggests that GABA neurotransmission is a promising target for treatment interventions of abnormal multisensory processing in clinical populations. In summary, our study provides strong evidence that the GABA level shapes individual differences in audiovisual perception through its modulatory influence on GBO.

Acknowledgments

This work was supported by grants from the German Research Foundation (GA707/6-1 to J.G., KE1828/2-1 to J.K., and SE1859/3-1 to D.S.) and the European Union (ERC-2010-StG-20091209 to D.S.). The hand

icon and speaker symbol in Fig. 1 were made by Freepik and Icon Works, respectively, from flaticon.com. We would like to thank Tobias Bernklau, Melissa Henjes, Markus Koch, and Paulina Schulz for their assistance in the data collection.

Conflict of interest

The authors report no potential conflicts of interest.

References

Andersen, T.S., Tiippana, K., Sams, M., 2004. Factors influencing audiovisual fission and fusion illusions. Brain Res. Cogn. Brain Res. 21, 301–308.

Attalah, B.V., Scanziani, M., 2009. Instantaneous modulation of gamma oscillation frequency by balancing excitation with inhibition. Neuron 62, 566–577.

Bartos, M., Vida, I., Jonas, P., 2007. Synaptic mechanisms of synchronized gamma oscillations in inhibitory interneuron networks. Nat. Rev. Neurosci. 8, 45–56.

Beauchamp, M.S., Argall, B.D., Bodurka, J., Duyn, J.H., Martin, A., 2004. Unraveling multisensory integration: patchy organization within human STS multisensory cortex. Nat. Neurosci. 7, 1190–1192.

Beauchamp, M.S., Nath, A.R., Pasalar, S., 2010. fMRI-guided transcranial magnetic stimulation reveals that the superior temporal sulcus is a cortical locus of the McGurk effect. J. Neurosci. 30, 2414–2417.

Bhattacharya, J., Shams, L., Shimojo, S., 2002. Sound-induced illusory flash perception: role of gamma band responses. Neuroreport 13, 1727–1730.

Brandwein, A.B., Foxe, J.J., Butler, J.S., Russo, N.N., Altschuler, T.S., Gomes, H., Molholm, S., 2013. The development of multisensory integration in high-functioning autism: high-density electrical mapping and psychophysical measures reveal impairments in the processing of audiovisual inputs. Cereb. Cortex 23, 1329–1341.

Buckholtz, J.W., Treadway, M.T., Cowan, R.L., Woodward, N.D., Li, R., Ansari, M.S., Baldwin, R.M., Schwartzman, A.N., Shelby, E.S., Smith, C.E., Kessler, R.M., Zald, D.H., 2010. Dopaminergic network differences in human impulsivity. Science 329, 532.

Buzsáki, G., Wang, X.-J., 2012. Mechanisms of gamma oscillations. Annu. Rev. Neurosci. 35, 203–225.

Calvert, G., 2001. Crossmodal processing in the human brain: insights from functional neuroimaging studies. Cereb. Cortex 11, 1110–1123.

Cloke, J.M., Winters, B.D., 2015. alpha(4)beta(2) Nicotinic receptor stimulation of the GABAergic system within the orbitofrontal cortex ameliorates the severe crossmodal object recognition impairment in ketamine-treated rats: implications for cognitive dysfunction in schizophrenia. Neuropharmacology 90, 42–52.

Cousijn, H., Haegens, S., Wallis, G., Near, J., Stokes, M.G., Harrison, P.J., Nobre, A.C., 2014. Resting GABA and glutamate concentrations do not predict visual gamma frequency or amplitude. Proc. Natl. Acad. Sci. U. S. A. 111, 9301–9306.

Delorme, A., Makeig, S., 2004. EEGLAB: an open source toolbox for analysis of single-trial EEG dynamics including independent component analysis. J. Neurosci. Methods 134, 9–21.

Edden, R.A., Muthukumaraswamy, S.D., Freeman, T.C., Singh, K.D., 2009. Orientation discrimination performance is predicted by GABA concentration and gamma oscillation frequency in human primary visual cortex. J. Neurosci. 29, 15721–15726.

Edden, R.A.E., Intrapiromkul, J., Zhu, H., Cheng, Y., Barker, P.B., 2012. Measuring T2 in vivo with J-difference editing: application to GABA at 3 Tesla. J. Magn. Reson. Imaging 35, 229–234.

Gogolla, N., Takesian, A.E., Feng, G., Fagiolini, M., Hensch, T.K., 2014. Sensory integration in mouse insular cortex reflects GABA circuit maturation. Neuron 83, 894–905.

Gross, J., Kujala, J., Hamalainen, M., Timmermann, L., Schnitzler, A., Salmelin, R., 2001. Dynamic imaging of coherent sources: studying neural interactions in the human brain. Proc. Natl. Acad. Sci. U. S. A. 98, 694–699.

Hipp, J.F., Engel, A.K., Siegel, M., 2011. Oscillatory synchronization in large-scale cortical networks predicts perception. Neuron 69, 387–396.

Hoshino, O., 2012. Regulation of ambient GABA levels by neuron–glia signaling for reliable perception of multisensory events. Neural Comput. 24, 2964–2993.

Hoshino, O., 2014. Balanced crossmodal excitation and inhibition essential for maximizing multisensory gain. Neural Comput. 26, 1362–1385.

Isaacson, J.S., Scanziani, M., 2011. How inhibition shapes cortical activity. Neuron 72, 231–243.

Iurilli, G., Ghezzi, D., Olcese, U., Lassi, G., Nazzaro, C., Tonini, R., Tucci, V., Benfenati, F., Medini, P., 2012. Sound-driven synaptic inhibition in primary visual cortex. Neuron 73, 814–828.

Kaiser, J., Hertrich, I., Ackermann, H., Mathiak, K., Lutzenberger, W., 2005. Hearing lips: gamma-band activity during audiovisual speech perception. Cereb. Cortex 15, 646–653.

Kayser, C., Logothetis, N.K., 2009. Directed interactions between auditory and superior temporal cortices and their role in sensory integration. Front. Integr. Neurosci. 3, 7.

Keil, J., Müller, N., Hartmann, T., Weisz, N., 2014. Prestimulus beta power and phase synchrony influence the sound-induced flash illusion. Cereb. Cortex 24, 1278–1288.

Lakatos, P., Chen, C.M., O'Connell, M.N., Mills, A., Schroeder, C.E., 2007. Neuronal oscillations and multisensory interaction in primary auditory cortex. Neuron 53, 279–292.

Lally, N., Mullins, P.G., Roberts, M.V., Price, D., Gruber, T., Haenschel, C., 2014. Glutamatergic correlates of gamma-band oscillatory activity during cognition: a concurrent ER-MRS and EEG study. Neuroimage 85, 823–833.

Lange, J., Oostenveld, R., Fries, P., 2011. Perception of the touch-induced visual double-flash illusion correlates with changes of rhythmic neuronal activity in human visual and somatosensory areas. Neuroimage 54, 1395–1405.

Lange, J., Oostenveld, R., Fries, P., 2013. Reduced occipital alpha power indexes enhanced excitability rather than improved visual perception. J. Neurosci. 33, 3212–3220.

Lozano-Soldevilla, D., ter Huurne, N., Cools, R., Jensen, O., 2014. GABAergic modulation of visual gamma and alpha oscillations and its consequences for working memory performance. Curr. Biol. 24, 2878–2887.

Maris, E., Oostenveld, R., 2007. Nonparametric statistical testing of EEG- and MEG-data. J. Neurosci. Methods 164, 177–190.

Mekle, R., Mlynárik, V., Gambarota, G., Hergt, M., Krueger, G., Gruetter, R., 2009. MR spectroscopy of the human brain with enhanced signal intensity at ultrashort echo times on a clinical platform at 3 T and 7 T. Magn. Reson. Med. 61, 1279–1285.

Mescher, M., Merkle, H., Kirsch, J., Garwood, M., Gruetter, R., 1998. Simultaneous in vivo spectral editing and water suppression. NMR Biomed. 11, 266–272.

Mishra, J., Martinez, A., Sejnowski, T.J., Hillyard, S.A., 2007. Early cross-modal interactions in auditory and visual cortex underlie a sound-induced visual illusion. J. Neurosci. 27, 4120–4131.

Mlynarik, V., Gambarota, G., Frenkel, H., Gruetter, R., 2006. Localized short-echo-time proton MR spectroscopy with full signal-intensity acquisition. Magn. Reson. Med. 56, 965–970.

Muthukumaraswamy, S.D., Edden, R.A.E., Jones, D.K., Swettenham, J.B., Singh, K.D., 2009. Resting GABA concentration predicts peak gamma frequency and fMRI amplitude in response to visual stimulation in humans. Proc. Natl. Acad. Sci. U. S. A. 106, 8356–8361.

Nath, A.R., Beauchamp, M.S., 2012. A neural basis for interindividual differences in the McGurk effect, a multisensory speech illusion. Neuroimage 59, 781–787.

Near, J., Andersson, J., Maron, E., Mekle, R., Gruetter, R., Cowen, P., Jezzard, P., 2013. Unedited in vivo detection and quantification of gamma-aminobutyric acid in the occipital cortex using short-TE MRS at 3 T. NMR Biomed. 26, 1353–1362.

Noesselt, T., Rieger, J.W., Schoenfeld, M.A., Kanowski, M., Hinrichs, H., Heinze, H.J., Driver, J., 2007. Audiovisual temporal correspondence modulates human multisensory superior temporal sulcus plus primary sensory cortices. J. Neurosci. 27, 11431–11441.

Oostenveld, R., Fries, P., Maris, E., Schoffelen, J.M., 2011. FieldTrip: open source software for advanced analysis of MEG, EEG, and invasive electrophysiological data. Comput. Intell. Neurosci. 2011, 1–9.

Provencher, S.W., 1993. Estimation of metabolite concentrations from localized in vivo proton NMR spectra. Magn. Reson. Med. 30, 672–679.

Ross, L.A., Saint-Amour, D., Leavitt, V.M., Molholm, S., Javitt, D.C., Foxe, J.J., 2007. Impaired multisensory processing in schizophrenia: deficits in the visual enhancement of speech comprehension under noisy environmental conditions. Schizophr. Res. 97, 173–183.

Schneider, T.R., Lorenz, S., Senkowski, D., Engel, A.K., 2011. Gamma-band activity as a signature for cross-modal priming of auditory object recognition by active haptic exploration. J. Neurosci. 31, 2502–2510.

Senkowski, D., Schneider, T.R., Foxe, J.J., Engel, A.K., 2008. Crossmodal binding through neural coherence: implications for multisensory processing. Trends Neurosci. 31, 401–409.

Senkowski, D., Kautz, J., Hauck, M., Zimmermann, R., Engel, A.K., 2011. Emotional facial expressions modulate pain-induced beta and gamma oscillations in sensorimotor cortex. J. Neurosci. 31, 14542–14550.

Shams, L., Kamitani, Y., Shimojo, S., 2000. Illusions. What you see is what you hear. Nature 408, 788.

Sohal, V.S., Zhang, F., Yizhar, O., Deisseroth, K., 2009. Parvalbumin neurons and gamma rhythms enhance cortical circuit performance. Nature 459, 698–702.

Sumner, P., Edden, R.A.E., Bompas, A., Evans, C.J., Singh, K.D., 2010. More GABA, less distraction: a neurochemical predictor of motor decision speed. Nat. Neurosci. 13, 825–827.

Traub, R.D., Cunningham, M.O., Gloveli, T., LeBeau, F.E.N., Bibbig, A., Buhl, E.H., Whittington, M.A., 2003. GABA-enhanced collective behavior in neuronal axons underlies persistent gamma-frequency oscillations. Proc. Natl. Acad. Sci. U. S. A. 100, 11047–11052.

Tzourio-Mazoyer, B., Landeau, B., Papathanassiou, D., Crivello, F., Etard, O., Delcroix, N., Mazoyer, B., Joliot, M., 2002. Automated anatomical labeling of activations in SPM using a macroscopic anatomical parcellation of the MNI MRI single-subject brain. Neuroimage 15, 273–289.

Uhlhaas, P.J., Singer, W., 2012. Neuronal dynamics and neuropsychiatric disorders: toward a translational paradigm for dysfunctional large-scale networks. Neuron 75, 963–980.

Urbantschitsch, V., 1888. Ueber den Einfluss einer Sinneserregung auf die übrigen Sinnesempfindungen. Pflugers Arch. — Eur. J. Physiol. 42, 29.

Ursino, M., Cona, F., Zavaglia, M., 2010. The generation of rhythms within a cortical region: analysis of a neural mass model. Neuroimage 52, 1080–1094.

Van Atteveldt, N., Murray, M.M., Thut, G., Schroeder, C.E., 2014. Multisensory integration: flexible use of general operations. Neuron 81, 1240–1253.

Van Loon, A.M., Knapen, T., Scholte, H.S., St. John-Saaltink, E., Donner, T.H., Lamme, V.aF., 2013. GABA shapes the dynamics of bistable perception. Curr. Biol. 23, 823–827.

Van Veen, B.D., van Drongelen, W., Yuchtman, M., Suzuki, a, 1997. Localization of brain electrical activity via linearly constrained minimum variance spatial filtering. IEEE Trans. Biomed. Eng. 44, 867–880.

Wang, X.-J., 2010. Neurophysiological and computational principles of cortical rhythms in cognition. Physiol. Rev. 90, 1195–1268.

Wendling, F., Bartolomei, F., Bellanger, J.J., Chauvel, P., 2002. Epileptic fast activity can be explained by a model of impaired GABAergic dendritic inhibition. Eur. J. Neurosci. 15, 1499–1508.

Wetzels, R., Wagenmakers, E.-J., 2012. A default Bayesian hypothesis test for correlations and partial correlations. Psychon. Bull. Rev. 1057–1064.

Whittington, M.A., Traub, R.D., Jefferys, J.G., 1995. Synchronized oscillations in interneuron networks driven by metabotropic glutamate receptor activation. Nature 373, 612–615.